Inhibition of PKCδ reduces cisplatin-induced nephrotoxicity without blocking chemotherapeutic efficacy in mouse models of cancer

Navjotsingh Pabla,[1] Guie Dong,[1] Man Jiang,[1] Shuang Huang,[2] M. Vijay Kumar,[3] Robert O. Messing,[4] and Zheng Dong[1,3]

[1]Department of Cellular Biology and Anatomy and [2]Department of Biochemistry and Molecular Biology, Medical College of Georgia, Georgia Health Sciences University, Augusta, Georgia, USA. [3]Research Department, Charlie Norwood VA Medical Center, Augusta, Georgia, USA. [4]Ernest Gallo Clinic and Research Center, University of California, San Francisco, California, USA.

Cisplatin is a widely used cancer therapy drug that unfortunately has major side effects in normal tissues, notably nephrotoxicity in kidneys. Despite intensive research, the mechanism of cisplatin-induced nephrotoxicity remains unclear, and renoprotective approaches during cisplatin-based chemotherapy are lacking. Here we have identified PKCδ as a critical regulator of cisplatin nephrotoxicity, which can be effectively targeted for renoprotection during chemotherapy. We showed that early during cisplatin nephrotoxicity, Src interacted with, phosphorylated, and activated PKCδ in mouse kidney lysates. After activation, PKCδ regulated MAPKs, but not p53, to induce renal cell apoptosis. Thus, inhibition of PKCδ pharmacologically or genetically attenuated kidney cell apoptosis and tissue damage, preserving renal function during cisplatin treatment. Conversely, inhibition of PKCδ enhanced cisplatin-induced cell death in multiple cancer cell lines and, remarkably, enhanced the chemotherapeutic effects of cisplatin in several xenograft and syngeneic mouse tumor models while protecting kidneys from nephrotoxicity. Together these results demonstrate a role of PKCδ in cisplatin nephrotoxicity and support targeting PKCδ as an effective strategy for renoprotection during cisplatin-based cancer therapy.

Introduction

Cisplatin is one of the most widely used and most potent chemotherapeutic agents (1–4). It is being used for the treatment of testicular, ovarian, head and neck, and lung cancer as well as many other types of cancers. In combination with other therapeutics, cisplatin is particularly effective in treating testicular and ovarian cancer, with an impressive cure rate (1–4). However, the use of cisplatin is limited by its side effects in normal tissues, particularly nephrotoxicity (5–7). Although extensive hydration can reduce renal injury, over a quarter of patients still develop renal problems, leading to renal dysfunction and acute renal failure (5–7).

Cisplatin nephrotoxicity involves multiple factors and signaling pathways, culminating in renal tubular cell injury and death, and tissue damage (7–23). Despite intensive research, it remains unclear as to how these factors and pathways are regulated. Importantly, it is not known whether the same signaling pathways are also activated by cisplatin in cancer cells and contribute to its chemotherapeutic effects in tumors (7, 24). As a result, it remains to be determined whether it is possible to block pathways responsible for renal toxicity without diminishing the chemotherapeutic effect of cisplatin.

PKCδ is ubiquitously expressed in many cells and tissues (25–28). As a member of the novel PKC subfamily, PKCδ can be activated by diacylglycerol and phorbol esters in the absence of Ca^{2+}. Recent studies have further revealed additional mechanisms of PKCδ activation, which involve tyrosine phosphorylation and subcellular translocation (28). Functionally, PKCδ has been implicated in the regulation of a variety of cellular processes, ranging from signal transduction to apoptosis (25–31). Little is known about the regulation and involvement of PKCδ in renal pathophysiology.

In this study, we have identified PKCδ as a critical regulator of cisplatin nephrotoxicity. We show that PKCδ is activated by cisplatin via the tyrosine protein kinase Src. After activation, PKCδ may activate MAPKs to induce tubular cell injury and death. Pharmacological and genetic inhibition of PKCδ attenuates renal apoptosis and tissue damage, preserving renal function during cisplatin treatment. In cancer cells, however, inhibition of PKCδ may accelerate cell death during cisplatin treatment. Importantly, we found that inhibition of PKCδ enhanced the chemotherapeutic effects of cisplatin in several xenograft and syngeneic tumor models while protecting kidneys from nephrotoxicity. Together these studies identify what we believe to be a novel and effective strategy for renoprotection during cisplatin-based chemotherapy.

Results

PKCδ is activated during cisplatin treatment in renal proximal tubular cells and mouse kidneys. To analyze PKCδ activation during cisplatin nephrotoxicity, we used a well-characterized mouse model, in which a single dose of cisplatin induces acute kidney injury and renal failure (32–35). We first analyzed PKCδ activity using an in vitro kinase assay. PKCδ was immunoprecipitated from kidney tissue lysates and added to a kinase reaction buffer containing p^{32}-ATP and histone H1 as a substrate. As shown in Figure 1A, cisplatin treatment for 1 to 3 days led to 2- to 3-fold increases in PKCδ kinase activity in renal tissues. The increase was detected at day 1 of cisplatin treatment, a time point prior to kidney injury,

Conflict of interest: The authors have declared that no conflict of interest exists.
Citation for this article: *J Clin Invest.* 2011;121(7):2709–2722. doi:10.1172/JCI45586.

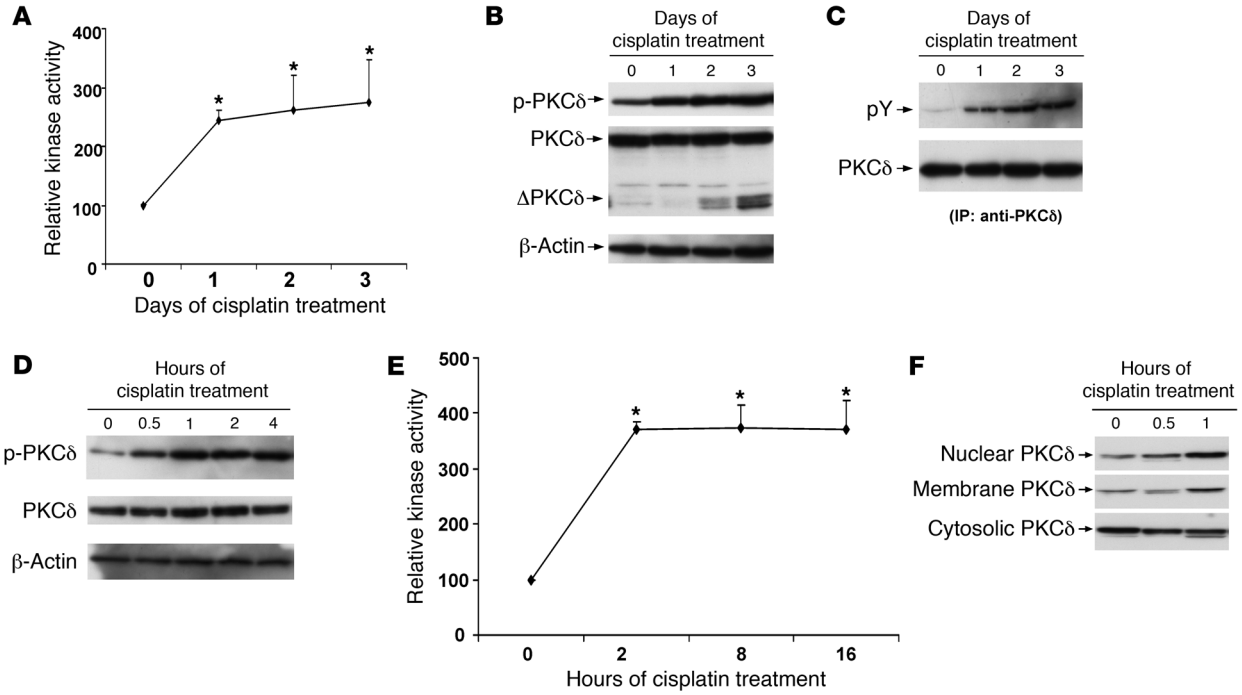

Figure 1

PKC-δ activation during cisplatin treatment in mice and RPTCs. (**A**) Kinase assay of PKCδ activity in kidney tissues. Male C57BL/6 mice of 8 to 10 weeks of age were injected with 30 mg/kg cisplatin before collection of renal tissues at day 0–3. PKCδ was immunoprecipitated from tissue lysate and in vitro kinase reaction with the substrate histone H1 and [γ-32P]ATP. Histone H1 phosphorylation was analyzed by SDS-PAGE and autoradiography to indicate kinase activity. (**B**) PKCδ phosphorylation at tyr-311 in kidney tissues. Kidney tissue lysate was analyzed by immunoblot analysis for phosphorylated (tyr-311) PKCδ (p-PKCδ), total PKCδ, or β-actin. (**C**) Tyrosine phosphorylation of PKCδ during cisplatin treatment in vivo. PKCδ was immunoprecipitated from control and cisplatin-treated renal tissues for immunoblot analysis of phosphotyrosine (pY). (**D**) PKCδ (tyr-311) phosphorylation during cisplatin treatment in vitro. RPTCs were treated with 20 μM cisplatin for 0 to 4 hours to collect whole cell lysates for immunoblot analysis of total and phosphorylated (tyr-311) PKCδ. (**E**) In vitro kinase assay of PKCδ activation in RPTCs. RPTCs were treated with 20 μM cisplatin for 0 to 16 hours to collect whole cell lysates for PKCδ immunoprecipitation and kinase activity assay. (**F**) Translocation of PKCδ during cisplatin treatment. RPTCs were treated with cisplatin for 0 to 1 hours and then fractionated into nuclear, membrane, and cytosolic fractions for immunoblot analysis of PKCδ. Mean ± SD, $n = 4$. *$P < 0.001$ versus control.

and continued to day 3, when severe kidney injury and renal failure developed (time course of renal injury is shown below). A representative blot of the in vitro kinase assay is shown in Supplemental Figure 1A (supplemental material available online with this article; doi:10.1172/JCI45586DS1). The increase of kinase activity after cisplatin treatment was not due to higher PKCδ expression, as the level of total PKCδ remained largely constant (Figure 1B). After 2 to 3 days of cisplatin treatment, PKCδ was partially cleaved, releasing detectable fragments (Figure 1B). It has been suggested that caspase-mediated cleavage of PKCδ may contribute to PKCδ activation by removing the autoinhibitory domain from the catalytic site (36). Nevertheless, in our study PKCδ was activated at day 1, prior to the proteolytic cleavage, suggesting an early proteolysis-independent mechanism for PKCδ activation during cisplatin nephrotoxicity. A newly discovered mechanism of PKCδ activation involves tyrosine phosphorylation and subcellular translocation (28). We detected PKCδ phosphorylation at tyr-311, which started at day 1 of cisplatin treatment and continued to day 3 (Figure 1B). We further immunoprecipitated PKCδ and analyzed its tyrosine phosphorylation using an antiphosphotyrosine antibody (pY). As shown in Figure 1C, cisplatin induced tyrosine phosphorylation of PKCδ in a time-dependent manner. In cultured renal proximal tubular cells (RPTCs), cisplatin also induced a rapid PKCδ phosphorylation and activation (Figure 1, D and E, and Supplemental Figure 1B). Nuclear translocation of PKCδ has been shown to be essential for its cytotoxic or proapoptotic function (37). Consistent with this finding, we detected PKCδ translocation to the nucleus during cisplatin treatment of RPTCs (Figure 1F and Supplemental Figure 1C). Together, these in vitro and in vivo analyses demonstrate an early PKCδ activation during cisplatin nephrotoxicity.

Src interacts with, phosphorylates, and activates PKCδ during cisplatin nephrotoxicity. To identify the protein kinase(s) that is responsible for PKCδ phosphorylation and activation during cisplatin nephrotoxicity, we screened pharmacological inhibitors of various tyrosine kinases. PP1 and PP2, two inhibitors of the Src family tyrosine kinase, suppressed cisplatin-induced PKCδ (tyr-311) phosphorylation, while the control compound PP3 had no effect (Figure 2A). Importantly, PP1 and PP2, but not PP3, abolished PKCδ activation during cisplatin treatment (Figure 2B), suggesting an important role for Src family kinases in PKCδ phosphorylation and activation. Mechanistically, we showed using coimmunoprecipitation that Src interacted with PKCδ in control RPTCs, and the molecular interaction was enhanced during cisplatin treatment (Figure 2C). Notably, the cisplatin-induced Src/PKCδ interaction was partially inhibited by PP1 and PP2 but not by PP3 (Figure 2C). The Src/PKCδ interaction was also shown during cisplatin nephrotoxicity

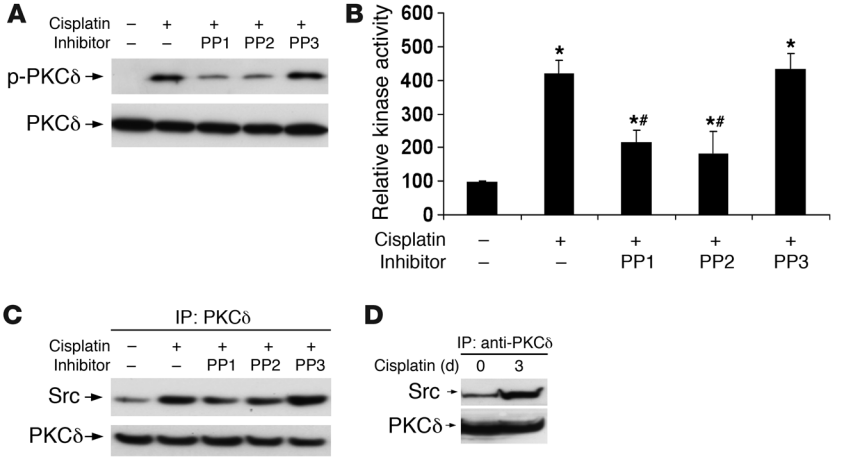

Figure 2

The role of Src in cisplatin-induced PKCδ activation. RPTCs were treated with 20 μM cisplatin for 4 hours in the absence or presence of 20 μM Src inhibitors, PP1 and PP2, or the control compound PP3. (**A**) Inhibition of PKCδ (tyr-311) phosphorylation during cisplatin treatment by Src inhibitors. Whole cell lysates were collected for immunoblotting of phosphorylated (tyr-311) PKCδ and total PKCδ. (**B**) Inhibition of PKCδ activity during cisplatin treatment by Src inhibitors. Whole cell lysates were collected for PKCδ immunoprecipitation and in vitro kinase assay. Mean ± SD, $n = 4$. $^*P < 0.001$ versus control; $^{\#}P < 0.001$ versus cisplatin-only group. (**C**) Coimmunoprecipitation of Src and PKCδ. Whole cell lysates were collected for immunoprecipitation of PKCδ. The immunoprecipitates were analyzed for the presence of Src and PKCδ by immunoblotting. (**D**) Coimmunoprecipitation of Src and PKCδ during cisplatin nephrotoxicity in vivo. C57BL/6 mice were injected with 30 mg/kg cisplatin before collection of renal tissues at days 0 and 3. The tissue lysates were immunoprecipitated using an anti-PKCδ antibody, and the immunoprecipitates were examined for Src and PKCδ by immunoblotting.

in vivo in mouse kidneys (Figure 2D). Collectively, these results suggest that PKCδ is activated by Src during cisplatin nephrotoxicity via molecular interaction and tyrosine phosphorylation.

Inhibition of PKCδ attenuates cisplatin-induced apoptosis in renal tubular cells and nephrotoxicity in mice. A role for PKCδ in cisplatin nephrotoxicity was first suggested by the cytoprotective effect of rottlerin, a pharmacological inhibitor of PKCδ. As shown in Figure 3A, cisplatin induced significant apoptosis in RPTCs, which was inhibited by rottlerin. The morphological observation was confirmed by flow cytometric quantification of apoptotic cells after Annexin V–FITC/propidium iodide (Annexin V–FITC/PI) staining (Figure 3B). During cisplatin treatment, apoptosis increased from 5.1% to 51.6%, which was suppressed to 21.6% by rottlerin. Apoptosis was also suppressed by bisindolylmaleimide I (BisI), a broad-spectrum PKC inhibitor, but not by Gö6976, an inhibitor of classic PKCs (Figure 3B). By cellular fractionation and immunoblot analysis, we further showed that rottlerin could inhibit the critical mitochondrial events of apoptosis, namely Bax translocation and cytochrome *c* release. As shown in Figure 3C, during cisplatin treatment, Bax translocated into mitochondria, accompanied by cytochrome *c* release from the organelles. Both Bax translocation and cytochrome *c* release were suppressed by rottlerin (Figure 3C). Rottlerin did not affect cisplatin uptake in these cells (data not shown). Concerning the specificity of rottlerin (38), we further determined the effects of dominant-negative PKCδ (PKCδ–kinase dead [PKCδ-KD]), which suppressed cisplatin-induced apoptosis, while dominant-negative PKCα (PKCα–kinase dead [PKCα-KD]) or the catalytic active PKCδ fragment (PKCδ-CF) were without effect (Figure 3D). The expression of PKCα, PKCβ, and PKCε did not change significantly during cisplatin nephrotoxicity in mice, and inhibition of these PKC isoforms by expression of dominant-negative mutants did not significantly affect cisplatin-induced apoptosis in RPTCs (Supplemental Figure 2).

The protective effects of rottlerin shown in vitro in cultured renal tubular cells were further demonstrated in vivo in C57BL/6 mice. As shown in Figure 4, A and B, cisplatin induced acute renal failure in the animals in 3 days, increasing blood urea nitrogen (BUN) to 220 mg/kg and serum creatinine to 1.8 mg/kg. The BUN and creatinine increases were partially but significantly attenuated by rottlerin. Consistently, rottlerin suppressed cisplatin-induced renal tissue damage and apoptosis (Figure 4, C and D). In this experiment, rottlerin inhibited PKCδ but not PKCα, supporting the specificity of rottlerin in renal cells and tissues (Supplemental Figure 3).

Cisplatin nephrotoxicity is attenuated in Pkcd$^{-/-}$ mice and renal tubular cells. To further establish the role of PKCδ in cisplatin nephrotoxicity, we examined *Pkcd*$^{-/-}$ mice (39); PKCδ deficiency in renal tissues of these animals was confirmed by immunoblot analysis (Supplemental Figure 4). *Pkcd*$^{-/-}$ mice and wild-type littermates were injected with 30 mg/kg cisplatin. At day 3, wild-type mice developed severe renal failure as shown by high levels of BUN (176 mg/dl) and serum creatinine (1.8 mg/dl). In contrast, *Pkcd*$^{-/-}$ mice showed significantly ($P < 0.05$) better renal function, with BUN levels of 85 mg/dl and serum creatinine levels of 0.9 mg/dl (Figure 5, A and B). These animals also showed a better renal histology and less apoptosis than wild-type mice (Figure 5, C and D). The tissue damage scores were 3.2 for wild-type mice and 1.8 for *Pkcd*$^{-/-}$ mice treated with cisplatin (Figure 5C). The resistance to renal injury observed in rottlerin-treated and PKCδ-deficient mice was not due to reduced renal uptake of cisplatin (Supplemental Figure 5). We further isolated proximal tubular cells from *Pkcd*$^{-/-}$ mice and their wild-type littermates for primary culture and examined cisplatin-induced apoptosis in these cells. As shown Figure 5E, cisplatin induced apoptosis in 72% of wild-type cells but in only 36% of *Pkcd*$^{-/-}$ proximal tubular cells. Cisplatin-induced caspase activation was also lower in *Pkcd*$^{-/-}$ cells (Figure 5F). Together the results indicate that PKCδ is an important regulator of cisplatin-induced tubular cell apoptosis, kidney injury, and renal failure.

Independent regulation of p53 and PKCδ during cisplatin nephrotoxicity. To delineate the signaling pathway downstream of PKCδ, we initially focused on p53, a tumor suppressor protein that was recently implicated in cisplatin-induced renal cell apoptosis and nephrotoxicity (34, 40–47). As shown in Figure 6A, cisplatin induced p53 (ser-15) phosphorylation in both wild-type and *Pkcd*$^{-/-}$ mice. Moreover, PUMA-α, the product of a p53-regulated apoptotic gene, was induced at similar levels in both genotypes. The in vivo results were confirmed in primary kidney proximal tubular cells isolated from wild-type and *Pkcd*$^{-/-}$ mice. As shown in Figure 6B, whether PKCδ was present or not, cisplatin induced p53 phosphorylation in these

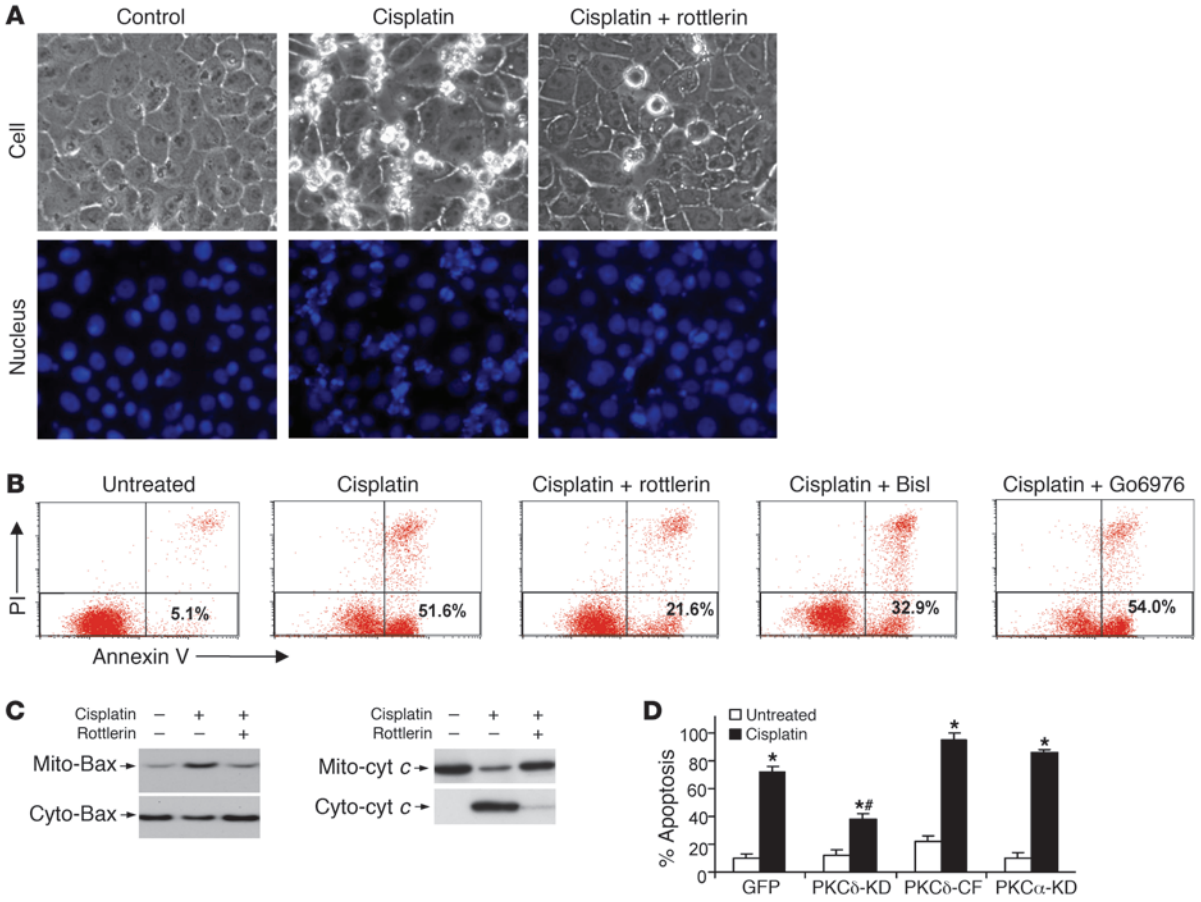

Figure 3

Effects of PKCδ inhibition on cisplatin-induced apoptosis in RPTCs. (**A**–**C**) RPTCs were treated with 20 μM cisplatin for 16 hours in the absence or presence of 10 μM rottlerin, BisI, or Go6976. (**A**) Morphology. After treatment, cells were stained with Hoechst33342. Cellular and nuclear morphology was recorded by phase-contrast and fluorescence microscopy. Original magnification, ×400. (**B**) Flow cytometric analysis of apoptosis. After treatment, cells were stained with Annexin V–FITC and PI for flow cytometry. Values in the plots represent percentages of Annexin V–FITC–positive cells. (**C**) Inhibition of Bax translocation and cytochrome *c* (cyt *c*) release during cisplatin treatment by rottlerin. Cells were fractionated into cytosolic (cyto) and membrane-bound organellar fractions for immunoblot analysis of Bax and cytochrome *c*. Mito, mitochondria. (**D**) Inhibition of cisplatin-induced apoptosis by dominant-negative PKCδ. RPTCs were cotransfected with pEGFP-C3 and a PKC plasmid (PKCδ-KD, PKCδ-CF, or PKCα-KD), and then treated with 20 μM cisplatin for 16 hours. Transfected cells (expressing GFP) were examined for the percentage of apoptosis by morphological criteria. Mean ± SD, $n = 4$. $^*P < 0.05$ versus untreated control cells, $^{\#}P < 0.05$ versus cisplatin-treated GFP/empty vector–transfected cells.

primary cells. We further showed that PKCδ (tyr-311) phosphorylation was independent of p53 in kidney tissues (Figure 6C) and also in primary kidney tubular cells (Figure 6D). Thus PKCδ and p53 appeared to be independently regulated during cisplatin nephrotoxicity. Functionally, cisplatin-induced apoptosis in *Pkcd*$^{-/-}$ cells could be further suppressed by pifithrin-α, a pharmacological inhibitor of p53, whereas rottlerin (an inhibitor of PKCδ) was not effective (Figure 6E). On the other hand, rottlerin, but not pifithrin-α, could suppress cisplatin-induced apoptosis in *p53*$^{-/-}$ cells (Figure 6F). The additive effects of PKCδ and p53 inhibitions further suggest that PKCδ and p53 function in separate pathways to promote renal cell apoptosis and cisplatin nephrotoxicity. Of note, the PKCδ- and p53-mediated signaling pathways are not the only signaling pathways responsible for cisplatin nephrotoxicity, because 20%–30% apoptosis remained, even under the conditions of inhibition of both PKCδ and p53 (Figure 6, E and F).

MAPKs are downstream of PKCδ in apoptotic signaling during cisplatin nephrotoxicity. We further determined the involvement of MAPKs in PKCδ signaling during cisplatin nephrotoxicity. MAPKs, including ERK, JNK, and p38, contribute to cisplatin-induced kidney cell apoptosis and renal failure (11, 19, 22, 48, 49). However, it is not entirely clear how MAPKs are activated under the pathological condition. Consistent with previous studies, we detected the activation of JNK, ERK, and p38 MAPK in kidney tissues from cisplatin-treated wild-type C57BL/6 mice (Figure 7A). Interestingly, JNK and ERK activation started from day 1 of cisplatin treatment and lasted to day 3, whereas p38 activation was transient and only detected at day 2. In *Pkcd*$^{-/-}$ mouse kidneys, cisplatin-induced JNK activation was markedly delayed (to day 3), and p38 activation was completely abolished, while ERK activation was transiently suppressed at day 2 (Figure 7A). Consistently, cisplatin-induced MAPK activation was markedly diminished in primary kidney proximal

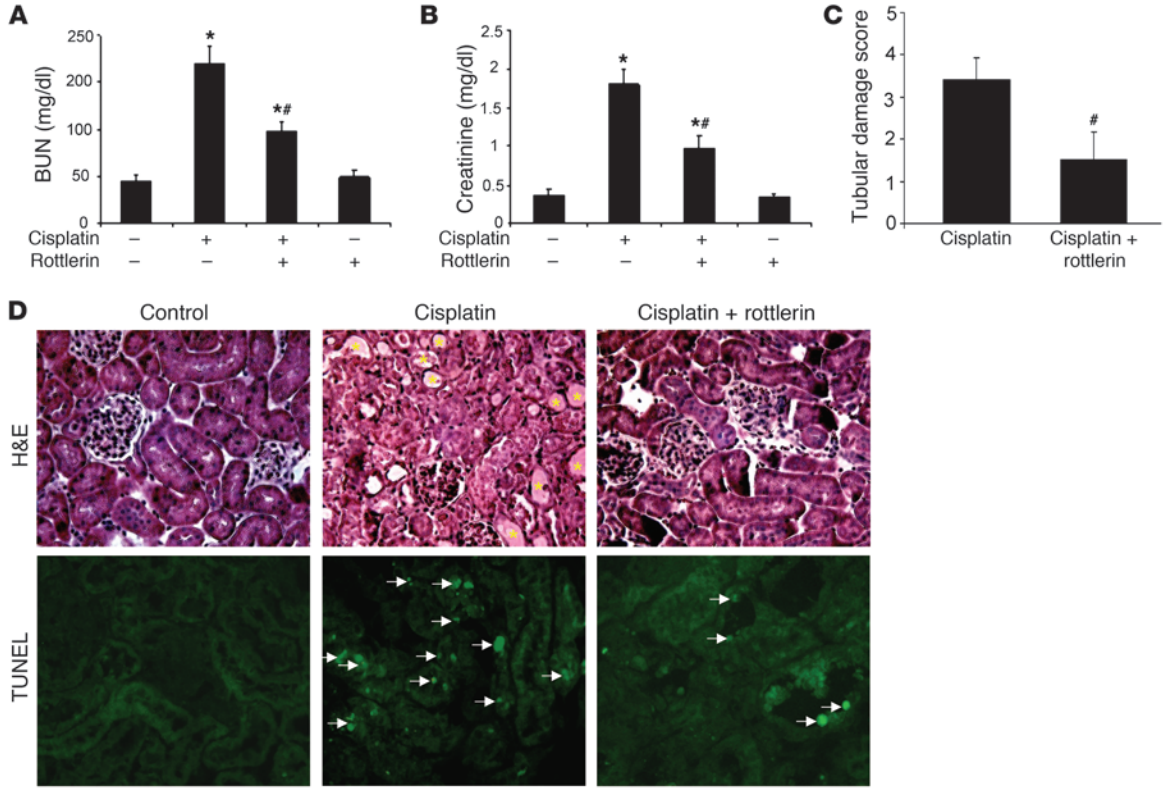

Figure 4

Effects of rottlerin on cisplatin-induced nephrotoxicity in vivo in mice. Male C57BL/6 mice of 8 to 10 weeks of age were injected with saline (control), 30 mg/kg cisplatin, 30 mg/kg cisplatin plus 10 mg/kg rottlerin, or 10 mg/kg rottlerin. Blood samples were collected at day 3 to measure (**A**) BUN and (**B**) serum creatinine. Renal tissues were also collected and processed for H&E staining to evaluate (**C**) tubular damage and (**D**) histology. Mean ± SD, $n = 4$. *$P < 0.001$ versus untreated control group; #$P < 0.05$ versus cisplatin-only group. (**D**) Apoptosis was examined by TUNEL assay. Arrows indicate TUNEL-positive nuclei. Original magnification, ×200.

tubular cells isolated from *Pkcd*$^{-/-}$ mice (Figure 7B), further suggesting that MAPKs may be downstream of PKCδ signaling during cisplatin nephrotoxicity. Using the primary cells, we then determined the effects of MAPK inhibitors (SP600125 for JNK, U0126 for ERK, SB203580 for p38) on cisplatin-induced apoptosis; inhibition of respective MAPKs by these inhibitors was confirmed by analyzing MAPK phosphorylation (Figure 7B, lane 24+I). In wild-type tubular cells, all 3 MAPK inhibitors suppressed cisplatin-induced apoptosis (Figure 7C). Nevertheless, in *Pkcd*$^{-/-}$ cells, only the ERK inhibitor U0126 was inhibitory ($P < 0.05$). The additive effects of PKCδ deficiency and ERK inhibition on apoptosis suggest that PKCδ and ERK may promote cisplatin nephrotoxicity via separate pathways. On the other hand, the lack of additive effects of PKCδ deficiency and JNK/p38 inhibition suggest that JNK/p38 may be downstream of PKCδ in the signaling pathway, leading to tubular cell apoptosis during cisplatin nephrotoxicity.

Effects of PKCδ inhibition on cisplatin-induced apoptosis in cancer cells. The identification of PKCδ as a key regulator of cisplatin nephrotoxicity (Figures 1–7) suggested that it was possible to target PKCδ for renoprotection during cisplatin-based cancer therapy. However, there was a critical question: will PKCδ inhibition also diminish the cytotoxic or therapeutic effects of cisplatin in cancer cells and tumors? To address this, we initially examined the effects of rottlerin on cisplatin-induced apoptosis in multiple cancer cells in vitro (Supplemental Figure 6). Rottlerin markedly increased apoptosis during cisplatin treatment in all cancer cell lines tested. In these cells, cisplatin activated PKCδ, and the activation was inhibited by rottlerin (Supplemental Figure 7). The peptide PKCδ inhibitor δV1-1 also increased cisplatin-induced apoptosis in cancer cells (Figure 8A). To verify the pharmacological observation, we further analyzed the effects of dominant-negative PKCδ and PKCδ siRNA. As shown in Figure 8B, dominant-negative PKCδ and PKCδ siRNA increased cisplatin-induced apoptosis in several cancer cell lines, especially in MDA231 human breast cancer cells. The silencing effect of PKCδ siRNA was confirmed by immunoblot analysis (data not shown).

Rottlerin protects kidneys without diminishing the anticancer efficacy of cisplatin in human ovarian tumor xenografts. The distinct responses of kidney cells and cancer cell lines to PKCδ inhibition supported the feasibility of targeting PKCδ for renoprotection during cisplatin chemotherapy. To directly test this possibility, we first used a tumor xenograft model, in which A2780 human ovarian cancer cells were inoculated subcutaneously in athymic nude mice. After tumor establishment, the animals were divided into 3 groups. One group was treated weekly with 10 mg/kg cisplatin, and another group was treated with 10 mg/kg cisplatin plus 10 mg/kg rottlerin, while the control group was given saline. During the observation period of 4 weeks, the saline control group showed continuous tumor growth, while the 2 drug-treated groups showed tumor shrinkage (Figure 9A).

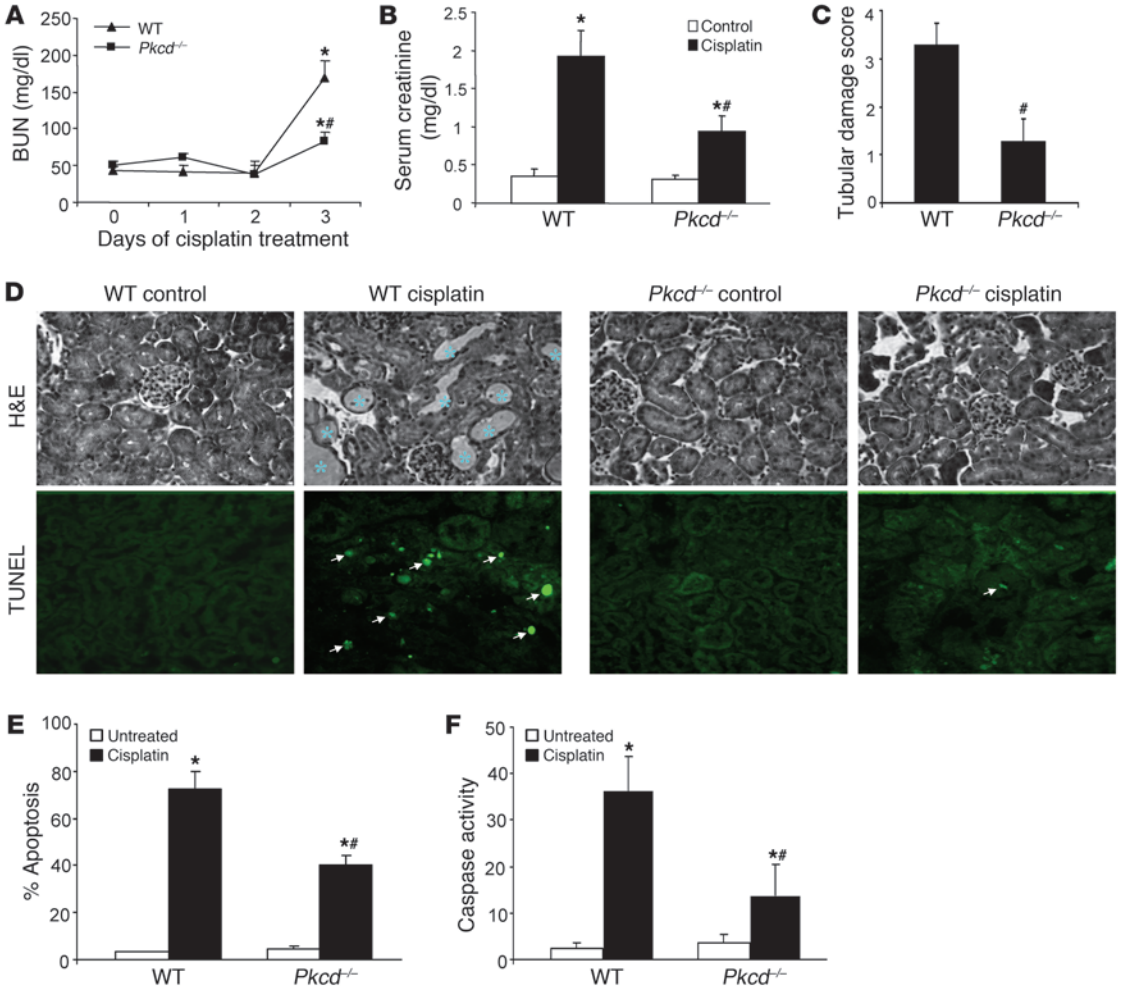

Figure 5

Resistance of *Pkcd*$^{-/-}$ mice and renal tubular cells to cisplatin-induced injury. (**A**–**D**) Wild-type and *Pkcd*$^{-/-}$ mouse littermates (male, 8–10 weeks of age) were injected with 30 mg/kg cisplatin. (**A**) Blood samples were collected at days 0, 1, 2, and 3 to measure BUN. At day 3, the animals were sacrificed to collect blood samples (**B**) to measure serum creatinine and (**C** and **D**) to collect kidney tissues for H&E staining and histological analysis and TUNEL assay of apoptosis. Asterisks in **D** indicate lysed tubules, and arrows indicate TUNEL-positive nuclei. Original magnification, ×200. (**E** and **F**) Kidney proximal tubular cells were isolated from wild-type and *Pkcd*$^{-/-}$ mice for primary culture. The cells were left untreated or treated with 30 μM cisplatin for 20 hours. Apoptosis was evaluated by cell morphology, and caspase activity was measured by enzymatic assay. Mean ± SD, $n = 4$. *$P < 0.001$ versus untreated control group; #$P < 0.05$ versus treated wild-type group.

At the end of 4 weeks, the average tumor weights were 5.78 g in the saline group, 0.44 g in the cisplatin group, and 0.39 g in the cisplatin plus rottlerin group (Figure 9, A and B). We further monitored renal function of these animals (Figure 9, C and D). Despite tumor growth, mice in the saline control group did not develop renal dysfunction as shown by low BUN and serum creatinine levels. In contrast, the cisplatin-treated group showed time-dependent increases in BUN and serum creatinine levels, which by the end of 4 weeks reached 179.6 for BUN and 2.2 mg/dl for creatinine. Notably, the group treated with cisplatin plus rottlerin had significantly ($P < 0.05$) better renal function. In this group, BUN and serum creatinine levels were not increased in the first 3 weeks, and by the end of 4 weeks, although an increase was detected, the level of increase was significantly ($P < 0.05$) lower than that of the cisplatin-only group (Figure 9, C and D). Furthermore, cisplatin-induced kidney tissue damage and apoptosis were ameliorated by coadministration of rottlerin (Figure 9E). The tissue damage score was 2.3 for the cisplatin-only group and 1.2 for the cisplatin plus rottlerin group. The beneficial effects of rottlerin were further substantiated by animal survival (Figure 9F). In the cisplatin-only group, animal death started at day 23 of treatment, and, within a week, 10 out of 11 animals died, with the last one dying at day 34. In the cisplatin plus rottlerin group, animal death was first noticed at day 30, and, within a week, 8 out of 11 animals expired. Nevertheless, 3 animals survived the entire observation period. Thus, in this xenograft model, animal death during cisplatin therapy was delayed overall and prevented in a subpopulation by rottlerin.

Rottlerin protects kidneys while enhancing the anticancer efficacy of cisplatin in a mouse syngenic ovarian tumor model. Inflammation, involving cross-talk between immune cells and renal parenchymal tissues, contributes significantly to cisplatin nephrotoxicity (6). In this regard, both T cells and dendritic cells may play important roles (50, 51).

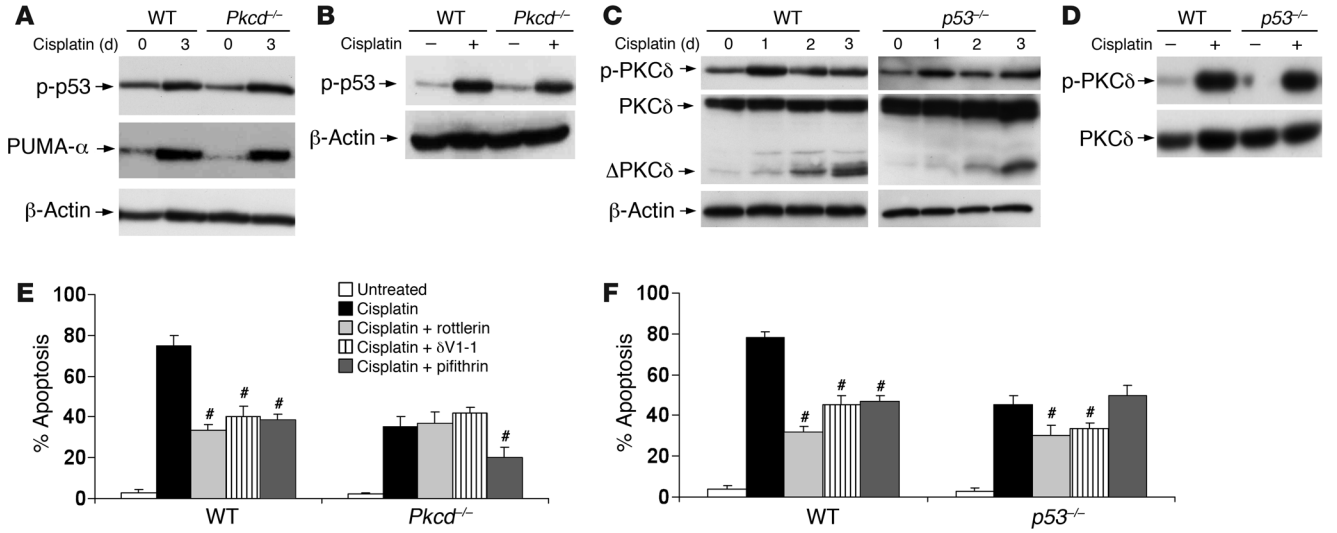

Figure 6

Independent regulation of p53 and PKCδ during cisplatin nephrotoxicity. (**A**) Cisplatin-induced p53 activation in kidney tissues. Wild-type and *Pkcd*$^{-/-}$ mice were injected with 30 mg/kg cisplatin before collection of whole kidney lysates for immunoblotting. (**B**) Cisplatin-induced p53 activation in primary *Pkcd*$^{-/-}$ kidney tubular cells. The cells were incubated with 50 μM cisplatin for 24 hours to collect lysate for immunoblotting. (**C**) Cisplatin-induced PKCδ activation in kidney tissues. Wild-type and *p53*$^{-/-}$ mice were injected with 30 mg/kg cisplatin before collection of whole kidney lysates for immunoblotting. (**D**) Cisplatin-induced PKCδ activation in primary *p53*$^{-/-}$ kidney tubular cells. The cells were incubated for 24 hours with 50 μM cisplatin to collect lysate for immunoblotting. (**E**) Effects of pifithrin-α and rottlerin on cisplatin-induced apoptosis in primary *Pkcd*$^{-/-}$ kidney tubular cells. The cells were treated for 24 hours with 50 μM cisplatin in the absence or presence of 10 μM rottlerin or 20 μM pifithrin-α to determine the percentage of apoptosis by morphological methods. (**F**) Effects of pifithrin-α and rottlerin on cisplatin-induced apoptosis in primary wild-type and *p53*$^{-/-}$ kidney tubular cells. The cells were treated for 24 hours with 50 μM cisplatin in the absence or presence of 10 μM rottlerin or 20 μM pifithrin-α to determine the percentage of apoptosis by morphological methods. Mean ± SD, $n = 4$. $^{\#}P < 0.05$ versus the cisplatin group of the same genotype cells.

However, the above xenograft model (Figure 9) used nude mice that were athymic and immune deficient. To determine whether immunodeficiency was a necessary factor for our results, we further examined a syngeneic tumor model in which tumors were established by injecting mouse ID8-VEGF ovarian cancer cells in immune-competent C57BL/6 mice (52). Compared with untreated animals, tumor growth was significantly suppressed by cisplatin alone and further inhibited by cisplatin plus rottlerin (Figure 10A). In terms of renal changes, cisplatin alone induced acute kidney injury, as indicated by progressive increases in BUN levels, which were markedly suppressed by cotreatment with rottlerin (Figure 10B). The cisplatin plus rottlerin–treated animals also showed less tubular damage (Figure 10C) and better renal histology (data not shown). Moreover, while all of the cisplatin-only–treated mice died within 4 weeks, approximately 40% of the animals of the cisplatin plus rottlerin group survived (Figure 10D). Of note, animal death in this and other tumor models (Figure 9) in the present study was caused by cisplatin and not by tumor growth, because animals without cisplatin treatment survived the whole observation period despite tumor growth (Figure 10D, untreated). Accordingly, the beneficial effect of rottlerin on animal death during cisplatin chemotherapy was attributable to its renoprotective effect.

PKCδ peptide inhibitor δV1-1 attenuates cisplatin nephrotoxicity while enhancing chemotherapy in testicular and breast cancer xenograft models. To extend our findings to another tumor type and test more specific PKCδ inhibitors, we examined the effects of δV1-1 in a testicular cancer xenograft model. δV1-1 is a PKCδ sequence-based peptide inhibitor that is conjugated to a Tat peptide for cell permeability and has been used in vivo to inhibit PKCδ activation under pathological conditions in the heart and brain (53–55). To establish testicular cancer xenografts, NCCIT cells were injected on both flanks of nude mice. In 2 weeks, the tumor volume increased to about 200 mm^3, and the mice were then divided into 5 groups for treatment: group I, saline (untreated); group II, cisplatin; group III, cisplatin plus rottlerin; group IV, cisplatin plus Tat peptide; and group V, cisplatin plus δV1-1. As shown in Figure 11A, untreated mice showed continuous tumor growth during the 4 weeks of observation, which was diminished in all other 4 groups. At the end of 4 weeks of treatment, the tumors in groups II–V were significantly smaller than those of the untreated group I. In addition, the tumors in mice from groups III and V were smaller than those in mice from groups II and IV, suggesting that rottlerin and δV1-1 might enhance the chemotherapeutic effect of cisplatin. BUN was determined to assess kidney injury. As shown in Figure 11B, BUN increased to 170 mg/dl in group II mice that were treated with cisplatin alone. Both rottlerin and δV1-1 suppressed the BUN increase, while the Tat peptide (a control for δV1-1) was not effective (Figure 11B). We further tested the effect of δV1-1 in a MDB-231 cell-based human breast cancer xenograft model. As shown in Figure 11C, cisplatin-induced reduction in tumor volume was further increased by cotreatment with δV1-1. In these animals, cisplatin nephrotoxicity was significantly ameliorated by δV1-1 (Figure 11D). Rottlerin and δV1-1 did not show significant renoprotective effects in PKCδ-deficient mice (Supplemental Figure 8), suggesting that these inhibitors are relatively specific in this experimental model. Cisplatin-induced weight loss in the tumor models was reduced by PKCδ inhibitors, indicating that these inhibitors may alleviate side effects of cisplatin in other organs, including the gastrointestinal

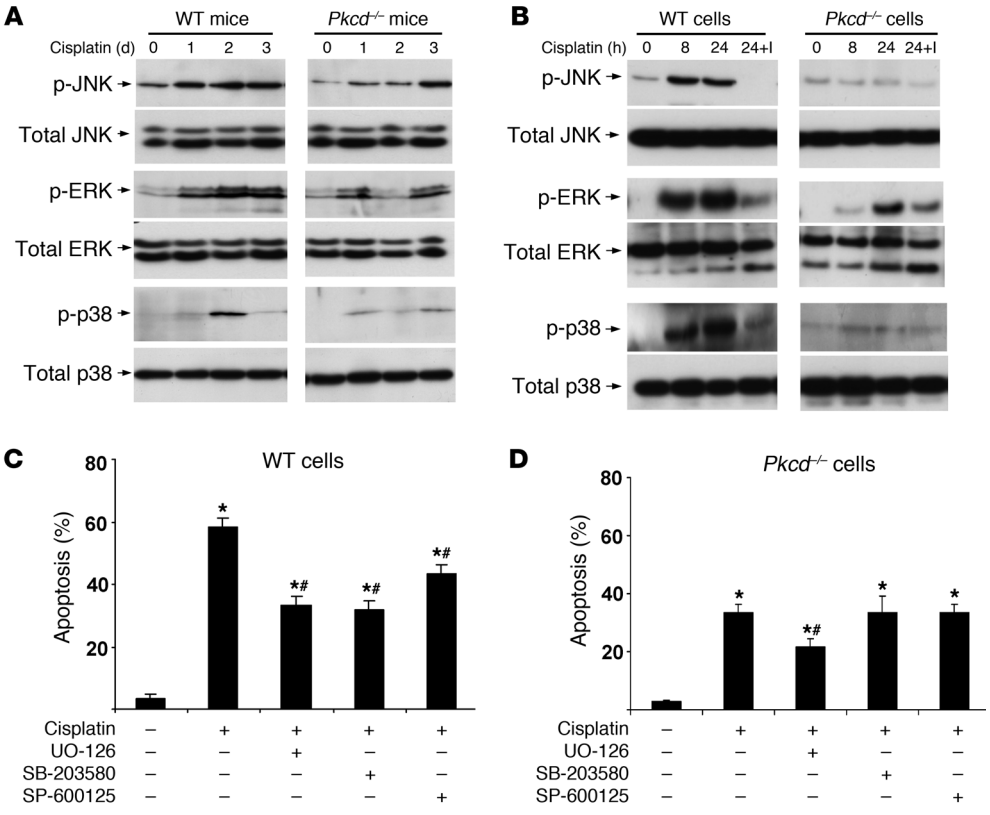

Figure 7

Regulation of MAPK by PKCδ during cisplatin nephrotoxicity. (**A**) MAPK activation during cisplatin nephrotoxicity in wild-type and *Pkcd*$^{-/-}$ mice. Male wild-type and *Pkcd*$^{-/-}$ mice of 8 to 10 weeks of age were injected with 30 mg/kg cisplatin. Whole kidney lysates were collected at days 0–3 for immunoblot analysis of phosphorylated and total JNK, ERK, and p38. (**B**) Cisplatin-induced MAPK activation in primary cultures of wild-type and *Pkcd*$^{-/-}$ kidney proximal tubular cells. The cells were incubated for 0, 8, 24 hours with 50 μM cisplatin or cisplatin and a MAPK inhibitor (24+I: 5 μM U0126, 10 μM SP600125, or 10 μM SB203580). Whole cell lysates were collected for immunoblot analysis of phosphorylated and total JNK, ERK, and p38. (**C** and **D**) Effects of MAPK inhibitors on cisplatin-induced apoptosis in wild-type and *Pkcd*$^{-/-}$ kidney proximal tubular cells. Kidney proximal tubular cells isolated from (**C**) wild-type and (**D**) *Pkcd*$^{-/-}$ mice were incubated for 24 hours with 50 μM cisplatin in the absence (–) or presence (+) of 5 μM U0126, 10 μM SP600125, or 10 μM SB203580. The percentage of apoptosis was determined by counting the cells with typical apoptotic morphology. Blots in **A** and **B** are representatives of at least 3 separate experiments. Mean ± SD, $n = 4$. *$P < 0.001$ versus untreated control group; #$P < 0.05$ versus cisplatin-only group.

tract (Supplemental Figure 9). Together with the ovarian tumor xenograft and syngeneic studies (Figures 8 and 9), these results demonstrate that inhibition of PKCδ can protect kidneys during cisplatin treatment, while maintaining or even enhancing the chemotherapeutic efficacy of cisplatin in certain tumor types.

Discussion

Nephrotoxicity is a major side effect that limits the use of cisplatin and its derivatives in cancer therapy. Over a quarter of patients receiving cisplatin treatment develop renal defects or acute kidney injury (5–7). Research during the last few years has demonstrated the activation of multiple signaling pathways during cisplatin nephrotoxicity, culminating in renal cell injury and death, tissue damage, and functional loss (11–23). Along with these studies, renoprotective approaches have been suggested. However, most of the studies examined cultured cells or tumor-free animal models, and, as a result, it remains unclear whether those reported renoprotective strategies would diminish the chemotherapeutic efficacy of cisplatin (7, 24). In the current study, we have identified PKCδ as a critical regulator of cisplatin-induced nephrotoxicity. Importantly, using both xenograft and syngeneic tumor models, we have shown that PKCδ inhibitors can protect kidneys from cisplatin-induced toxicity while preserving, and in some cases enhancing, cisplatin's chemotherapeutic effects. Together, these findings not only reveal what we believe to be a new signaling mechanism of cisplatin nephrotoxicity but identify an effective approach that we believe to be novel for renoprotection during cisplatin-based cancer therapy.

PKCδ as an important regulator of cisplatin-induced tubular cell apoptosis and acute kidney injury. Using both in vitro and in vivo models, we have demonstrated compelling evidence for a role of PKCδ in cisplatin nephrotoxicity. Importantly, the experiments used pharmacologic as well as genetic inhibitory approaches. Rottlerin and δV1-1, as pharmacological inhibitors of PKCδ, were shown to protect renal tubular cells against cisplatin-induced apoptosis (Figures 3 and 6). Moreover, these inhibitors protected against cisplatin nephrotoxicity in vivo in murine models (Figures 3 and 11). Genetically, cisplatin-induced apoptosis was inhibited by dominant-negative PKCδ (Figure 3D) and also by PKCδ deficiency in renal tubular cells (Figure 5, E and F). Notably, *Pkcd*$^{-/-}$ mice were markedly resistant to cisplatin-induced kidney injury, apoptosis, and renal failure (Figure 5, A–D). Of note, the resistance was not due to differences in cisplatin uptake (Supplemental Figure 5). Together, we believe these results have identified PKCδ as an important regulator of cisplatin nephrotoxicity.

Src as an upstream regulator of PKCδ during cisplatin nephrotoxicity. Like other novel PKCs, PKCδ can be activated by conventional mechanisms involving lipids and related cofactors. However, recent studies have revealed distinct mechanisms of PKCδ activation, involving subcellular translocation, proteolytic cleavage, and phosphorylation (25–31). In the current study, we detected an early PKCδ activation during cisplatin nephrotoxicity in vitro in cultured renal tubular cells and in vivo in C57BL/6 mice (Figure 1, A and E). The activation was associated with rapid tyrosine phosphorylation at tyr-311 and translocation of PKCδ to nuclear and

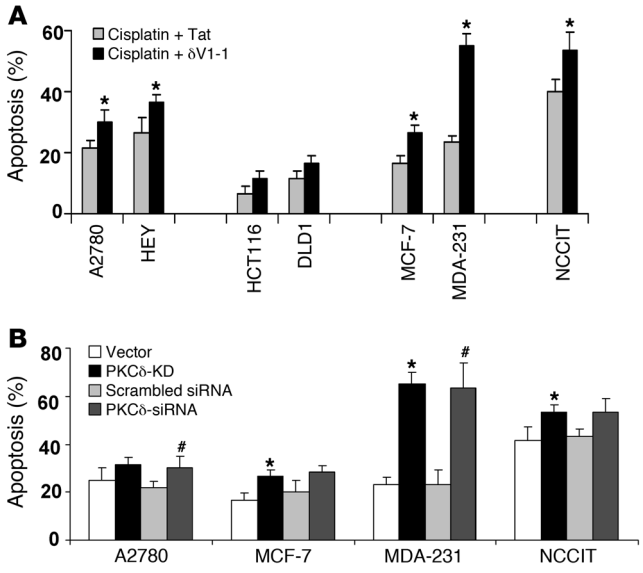

Figure 8
Effect of PKCδ inhibition on cisplatin-induced apoptosis in multiple cancer cell lines. (**A**) Effect of PKCδ inhibitor δV1-1 on cisplatin-induced apoptosis in cancer cells. Indicated cell lines were pretreated with 2 μM Tat or δV1-1 peptide for 1 hour in reduced serum medium before treating with 25 μM cisplatin for 24 hours, and apoptosis was monitored as described in Methods. Mean ± SD, $n = 3$. *$P < 0.05$ versus cisplatin plus Tat group. (**B**) Effect of genetic inhibition of PKCδ on cisplatin-induced apoptosis. Indicated cell lines were transfected with either empty vector, PKCδ-KD, scrambled siRNA, or PKCδ-siRNA, and 48 hours after transfection, the cells were treated with 20 μM cisplatin for 24 hours, and apoptosis was estimated. Mean ± SD, $n = 3$. *$P < 0.05$ versus vector group; #$P < 0.05$ versus scrambled siRNA group.

membrane fractions (Figure 1, B–D and F, and Supplemental Figure 1). In addition, PKCδ was proteolytically cleaved or processed at later time points (Figure 1B). Analyses of the time courses of the changes suggest that tyrosine phosphorylation and subcellular translocation contribute to early PKCδ activation, while proteolytic processing leads to additional activation at later time points. Furthermore, we showed that cisplatin-induced PKCδ activation can be mitigated by PP1 and PP2 but not by the control compound PP3 (Figure 2, A and B), suggesting that Src or a Src family kinase is upstream of PKCδ in the signaling cascade. Finally, our coimmunoprecipitation analysis showed that cisplatin treatment leads to an interaction between Src and PKCδ, and, notably, the molecular interaction is suppressed by PP1 and PP2 but not PP3 (Figure 2C), suggesting that Src may interact with and directly phosphorylate PKCδ, resulting in its activation. These observations are supportive of a newly proposed model of PKCδ activation, in which tyrosine phosphorylation by Src family kinases in the hinge region of PKCδ leads to autophosphorylation and activation PKCδ (28).

MAPKs, and not p53, as downstream mediators of PKCδ signaling during cisplatin nephrotoxicity. To understand the downstream signaling of PKCδ during cisplatin nephrotoxicity, we initially focused on p53. We hypothesized that PKCδ would phosphorylate p53, leading to p53 activation and consequent renal apoptosis. This hypothesis was mainly based on 2 considerations: (a) a role for p53 has been demonstrated in cisplatin nephrotoxicity (34, 40–47), and (b) PKCδ has recently been implicated in p53 phosphorylation and activation (56, 57). This hypothesis, seemingly logical, is nonetheless not supported by our results. In our study, cisplatin induced comparable levels of p53 activation in PKCδ-proficient and -deficient mice and tubular cells (Figure 6, A and B). Moreover, the activation of PKCδ was not affected by p53 deficiency (Figure 6, C and D). Importantly, we further demonstrated the additive effects of p53 and PKCδ inhibition on tubular cell apoptosis (Figure 6, E and F), suggesting that p53 and PKCδ may contribute to cisplatin nephrotoxicity via separate pathways.

In addition to p53, MAPKs are involved in cisplatin-induced renal cell apoptosis and nephrotoxicity. However, it is not fully understood how MAPKs are activated under this pathological condition (11, 19, 22, 48, 49). Our results have now demonstrated a role for PKCδ in MAPK activation during cisplatin treatment. In *Pkcd*$^{-/-}$ mice and tubular cells, cisplatin-induced MAPK (especially p38 and JNK) activation was markedly reduced (Figure 7, A and B). Notably, while JNK and p38 inhibitors suppressed apoptosis in wild-type tubular cells (Figure 7C), they could not reduce apoptosis in *Pkcd*$^{-/-}$ cells (Figure 7D). These results suggest that PKCδ regulates tubular cell apoptosis and cisplatin nephrotoxicity at least partly via MAPKs.

Targeting PKCδ as an effective renoprotective strategy during cisplatin-based cancer therapy. During the investigation of cisplatin nephrotoxicity, pharmacologic, molecular, and genetic approaches have been identified for renoprotection. However, most of the tests were conducted in cultured cells or tumor-free animals (see ref. 7 for a recent review). Whether these approaches would diminish the chemotherapeutic effects of cisplatin in cancers or tumors is unknown. This is particularly relevant because compromising the chemotherapy effects of cisplatin would jeopardize the primary goal of treatment. The present study, using both cultured cells and tumor-bearing animal models, demonstrates that inhibition of PKCδ can protect kidneys during cisplatin treatment while preserving and in some cases enhancing its anticancer efficacy, suggesting a novel and effective renoprotective approach.

Interestingly, previous studies have suggested that, depending on cell type, PKCδ may be proapoptotic or prosurvival (26). Of note, a prosurvival role of PKCδ has been documented in breast cancer, colon cancer, non–small cell lung carcinoma, chronic lymphocytic leukemia, and renal cell carcinoma cells (58–62). In breast cancer cells, PKCδ also promotes cell proliferation, migration, and metastasis (63–65). It has been recently suggested that due to the stress phenotype of cancer cells, nonessential proteins may become essential for their survival, a phenomenon termed "nononcogenic addiction" (66). PKCδ may be one of the prosurvival factors in some cancer or tumor types. Indeed, in our experiments, additional anticancer effects of PKCδ inhibitors (rottlerin and δV1-1) were demonstrated during cisplatin treatment of syngeneic ovarian tumors (Figure 10) and testicular and breast cancer xenografts (Figure 11). Together, these findings suggest that, depending on

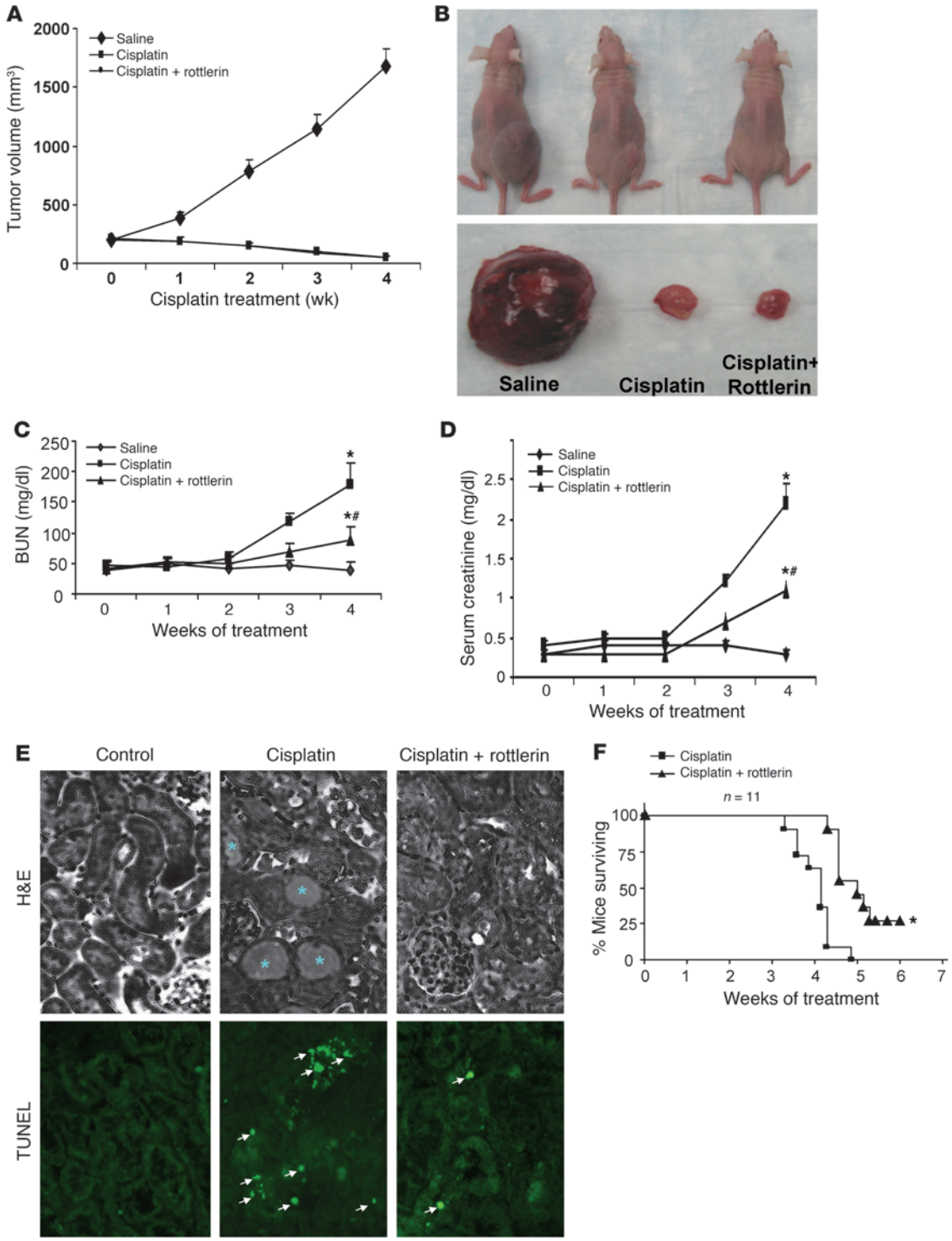

Figure 9

Rottlerin ameliorates cisplatin-induced kidney injury without blocking the therapeutic effects in human ovarian tumor xenografts. Tumor xenografts were established in athymic nude mice by inoculation of A2780 ovarian cancer cells. After the tumors had grown to approximately 200 mm^3, the animals were then randomly divided into 3 groups (11 mice/group), which were treated weekly with saline, 10 mg/kg cisplatin, or 10 mg/kg cisplatin plus 10 mg/kg rottlerin. (**A**) Tumor volume during treatment. Tumors were measured each week to determine tumor volume. (**B**) Representative mice and dissected tumors. (**C**) BUN values during the treatment. (**D**) Serum creatinine levels during the treatment. (**E**) Representative renal histology and TUNEL staining of tissues collected after 4 weeks of treatment. Original magnification, ×200. Asterisks in **E** indicate lysed tubules, and arrows indicate TUNEL-positive nuclei. (**F**) Animal death and survival during the treatment. Mean ± SD. $^*P < 0.05$ versus untreated saline control group; $^{\#}P < 0.05$ versus cisplatin-only group.

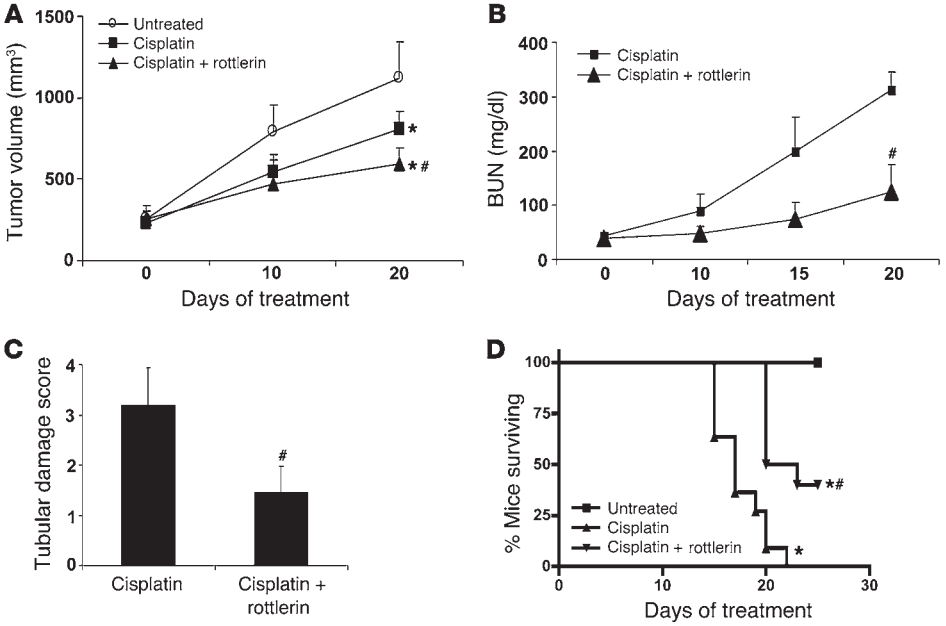

Figure 10
Rottlerin protects kidneys while enhancing cisplatin chemotherapy in syngeneic ovarian tumor model. C57BL/6 mice were injected subcutaneously with ID8-VEGF cells on the right flank. After the tumors had grown to approximately 200 mm^3, the mice were randomly divided into 3 treatment groups (10 mice/group): saline, 10 mg/kg cisplatin, or 10 mg/kg cisplatin plus 10 mg/kg rottlerin. (**A**) Tumor volume during treatment. (**B**) BUN levels during treatment. (**C**) Mice were sacrificed after 20 days of treatment to collect renal tissues for H&E staining and histological analysis. (**D**) Animal death and survival during cisplatin treatment. Mean ± SD (n = 10 for day 0–15 data, n = 3 for day 20 cisplatin data, n = 5 for day 20 cisplatin plus rottlerin data). *P < 0.05 versus untreated saline control group; #P < 0.01 versus cisplatin-only group.

the tumor type, PKCδ inhibition may not only protect kidneys but may also enhance the chemotherapeutic effect of cisplatin.

The specificity of rottlerin has been questioned recently (38). Therefore, we have established the role of PKCδ in cisplatin nephrotoxicity, not only by using rottlerin, but also by using dominant-negative mutants and gene knockout cells and animals (Figure 3D and Figure 5). In addition, rottlerin was shown to be protective in wild-type tubular cells but not in PKCδ-deficient cells (Figure 6E), confirming the PKCδ dependence of rottlerin's effect in these cells. In mouse kidney tissues, we further demonstrated that rottlerin specifically blocked the activation of PKCδ and not PKCα (Supplemental Figure 3). Importantly, in the testicular cancer xenograft model (Figure 11), we further established PKCδ as an effective target for renoprotection during cisplatin chemotherapy by demonstrating an effect of δV1-1, a sequence-based specific peptide inhibitor of PKCδ.

In conclusion, we believe we have identified PKCδ as a novel regulator of renal injury during cisplatin nephrotoxicity. PKCδ is activated during cisplatin treatment via Src phosphorylation and regulates MAPKs, leading to renal cell injury and death. Inhibition of PKCδ enhances the chemotherapeutic effects of cisplatin in several xenograft and syngeneic tumor models while protecting kidneys from nephrotoxicity. Targeting PKCδ may offer a new and effective strategy for renoprotection during cisplatin-based cancer therapy.

Methods

Reagents

The following antibodies were used: polyclonal anti-PKCδ from Calbiochem; polyclonal anti-phospho PKCδ (tyr-311) from Oncogene Research Products; polyclonal anti-p53, anti–phospho p53, and anti-PKCα from Cell Signaling Technology; monoclonal anti-Bax from NeoMarkers; monoclonal anti–cytochrome *c* from BD Pharmingen; monoclonal anti–β-actin from Sigma-Aldrich; polyclonal anti-PUMA from Jian Yu (University of Pittsburgh, Pittsburgh, Pennsylvania, USA); and all MAPK antibodies from New England Biolabs. Various PKC plasmids were obtained from Jae-Won Soh (Inha University, Inchun, Republic of Korea) and Fushin Yu (Wayne State University, Detroit, Michigan, USA). PKCδ-siRNA and scrambled siRNA were purchased from Dharmacom. δV1-1, the peptide inhibitor of PKCδ, was synthesized by the Microchemical Facility at Emory University, Atlanta, Georgia, USA, according to published protocol (53). The peptide inhibitor of caspases, VAD, and the fluorogenic peptide substrate of caspases, DEVD. AFC, were from Enzyme Systems Products. Histone H1 was from Santa Cruz Biotechnology and New England Biolabs. Rottlerin, BisI, Go6976, PP1, PP2, and PP3 were from Calbiochem. [γ-^{32}P]ATP was from MP Biochemicals. Other reagents, including, cisplatin were purchased from Sigma-Aldrich.

Animals and cells

Pkcd$^{-/-}$ C57BL/6 mice were generated by targeted gene deletion as described previously (39). *p53*$^{-/-}$ mice and wild-type C57BL/6 mice were from The Jackson Laboratory. Athymic nude mice (Foxn1^{nu}/Foxn1^{nu}) were from Harlan. All animals were housed in the animal facility of Charlie Norwood VA Medical Center. Animal experiments were conducted with the approval of and in accordance with the guidelines established by the Institutional Animal Care and Use Committee of Charlie Norwood VA Medical Center and Medical College of Georgia. The RPTC line was described previously (42, 44). Primary kidney proximal tubular cells were isolated and cultured as described recently (33, 34). A2780 cells were from T.C. Hamilton (Fox Chase Cancer Center, Philadelphia, Pennsylvania, USA). ID8 cells were from G. Coukos (University of Pennsylvania, Philadelphia, Pennsylvania, USA). HCT116 cells were from B. Vogelstein (Johns Hopkins University, Baltimore, Maryland, USA). Other cancer cell lines were purchased from ATCC.

Experimental models of cisplatin nephrotoxicity

In vivo, mice were injected with a single dose of 30 mg/kg cisplatin to induce kidney injury, as described recently (33–35). Control animals were injected with saline. In vitro, RPTCs and primary cultures of kidney proximal tubular cells were incubated with 20 μM and 30 μM cisplatin, respectively, which induced significant apoptosis and not necrosis as indicated previously (33, 34, 42, 44).

Tumor models

Ovarian tumor xenograft model. Female athymic nude mice of 7 to 8 weeks of age were inoculated by subcutaneous injection of 5 × 10^6 A2780 cells in 100 μl saline at the right flank. After inoculation, tumor growth was

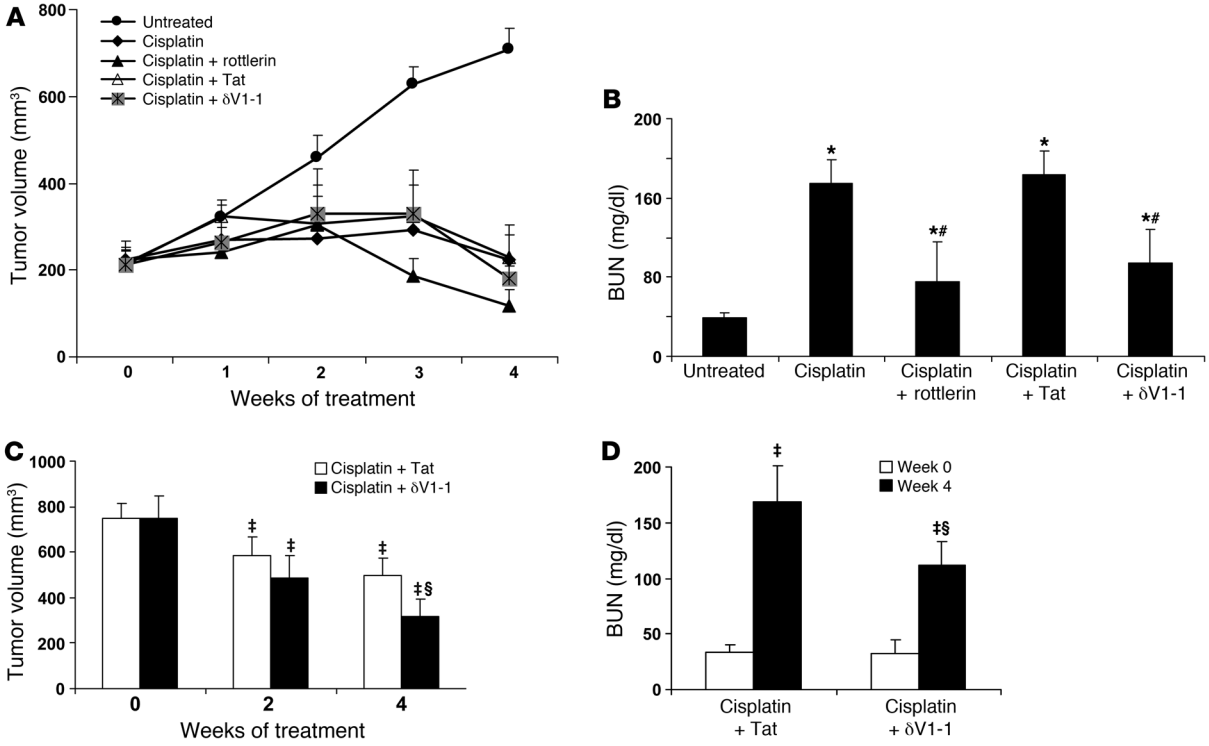

Figure 11

PKCδ inhibitor δV1-1 protect kidneys while enhancing cisplatin chemotherapy in human testicular and breast cancer tumor xenograft models. (**A** and **B**) Human NCCIT testicular cancer cells were injected into the flanks of 6- to 8-week-old male nude mice to monitor tumor growth. In 2 weeks, the tumor volume increased to approximately 200 mm^3, and the mice were divided into 5 groups (10 mice/group) for following treatments: saline (untreated), 20 mg/kg cisplatin, 20 mg/kg cisplatin plus 10 mg/kg rottlerin, 20 mg/kg cisplatin plus 3 mg/kg Tat peptide, and 20 mg/kg cisplatin plus 3 mg/kg δV1-1 peptide. Cisplatin and rottlerin were injected (i.p.) weekly. Tat and δV1-1 were injected (i.p.) biweekly. (**A**) Tumor volume. (**B**) BUN levels. (**C** and **D**) Human MDA-231 breast cancer cells were injected into the flanks of female nude mice. After the tumors grew to approximately 700 mm^3, the mice were treated with 10 mg/kg cisplatin plus 3 mg/kg Tat or 10 mg/kg cisplatin plus 3 mg/kg δV1-1. (**C**) Tumor volume and (**D**) BUN levels were measured at indicated times. Mean ± SD, $n = 6–10$. $^*P < 0.05$ versus untreated saline control group; $^‡P < 0.05$ versus week 0; $^{\#}P < 0.05$ versus cisplatin-only group; $^§P < 0.05$ versus cisplatin plus Tat group.

monitored for about 2 weeks with a vernier caliper. When the tumor size reached to approximately 200 mm^3, the animals were randomly divided into 3 groups for weekly i.p. treatment with cisplatin, cisplatin plus rottlerin, or saline as control. During the treatment, body weight and tumor size were monitored twice a week. BUN and serum creatinine levels were measured to monitor renal function.

Syngeneic ovarian tumor model. The model was slightly modified from Zhang et al. (52). ID8-VEGF cells were cultured, harvested, and suspended in PBS. Ten million cells were then injected subcutaneously into the right flank of 8-week-old C57BL/6 mice. The tumor size was measured using a Vernier caliper. After the tumor size reached approximately 200 mm^3, the mice were treated with saline, cisplatin, or cisplatin plus rottlerin. BUN and serum creatinine levels were measured to monitor renal function at indicated time points.

Testicular and breast tumor xenograft model. NCCIT cells (5×10^6 cells per site) or MDA-MB-231 cells (1×10^7 cells per site) were injected on both flanks of 6- to 8-week-old nude mice, and the tumor growth was routinely monitored using a Vernier caliper. In 2–3 weeks, the tumor volume increased to about 200 mm^3 (NCCIT) and 700 mm^3 (MDA-231), and the mice were divided into different groups for various treatments. Cisplatin and rottlerin were injected weekly by i.p. injection. Tat and δV1-1 were injected biweekly by i.p injection. Tumor volume was measured 2 times per week, and BUN was measured every week.

In vitro kinase assay of PKCδ and PKCα activities

The in vitro assay was modified from a recent study (67). Kidney tissues and cells were extracted with the IP lysis buffer containing 1% Triton X-100, in the presence of protease and phosphatase inhibitors. The lysates were subjected to immunoprecipitation using a specific antibody against PKCδ or PKCα. The immunoprecipitates were resuspended in the kinase reaction buffer containing 20 μM cold ATP and 20 μCi [γ-^{32}P]ATP and 100 μg/ml histone H1 for 15 minutes incubation at 30°C. After the incubation, 2% SDS was added to terminate the reaction. The samples were then subjected to gel electrophoresis and transferred to PVDF membranes. ^{32}P-labeled histone H1 was detected by autoradiography. Subsequently, the blots were immunoblotted for PKCδ or PKCα to confirm immunoprecipitation.

Coimmunoprecipitation of PKC-δ and Src

Kidney tissue and cell lysates were collected with the immunoprecipitation lysis buffer and subjected to immunoprecipitation using an anti-PKCδ or anti-Src antibody. The resultant precipitates were analyzed by gel electrophoresis and immunoblotting for Src and PKC-δ.

Analysis of apoptosis

Apoptosis in kidney tissues was analyzed by TUNEL assay using the In Situ Cell Death Detection Kit from Roche Applied Science, as described recently (33–35). Apoptosis in cell cultures was analyzed by standard methods,

including morphology, caspase activity, and Annexin V staining (42, 44, 68). For morphological analysis, cells were stained with Hoechst33342. The cells showing typical morphological features, including cellular and nuclear condensation and fragmentation, were counted to determine the percentage of apoptosis. Flow cytometric assay of apoptosis was performed, as described recently (44), using the Annexin V–FITC/PI staining kit from BD Biosciences. Briefly, cells were detached from the dishes by trypsinization and resuspended in the binding buffer containing Annexin V–FITC and PI. After 15 minutes of incubation at room temperature, the cells were diluted with binding buffer for analysis using a BD FACSCalibur flow cytometer (BD Biosciences). Over 10,000 events were counted for each sample.

Measurement of caspase activity

Caspase activity was measured by an enzymatic assay as previously described (42, 44, 68). Briefly, cells were lysed with a buffer containing 1% Triton X-100. The lysates of 25 μg protein were added to an enzymatic assay buffer containing 50 μM DEVD.AFC for 60 minutes at 37°C. Fluorescence at excitation 360 nm/emission 535 nm was measured with a GENios plate-reader (Tecan US Inc.). Free DEVD.AFC was used to plot a standard curve, and, using the standard curve, the fluorescence reading from the enzymatic reaction was converted into the nanomolar amount of DEVD.AFC liberated per mg protein per hour as a measure of caspase activity.

Cellular fractionation

To examine PKCδ translocation, cells were dounce homogenized on ice. The homogenates were sequentially centrifuged at 600 *g* for 10 minutes to collect the pellet as the nuclear fraction and at 14,000 *g* for 20 minutes to collect the pellet as the membrane fraction and the supernatant as the cytosolic fraction. To examine Bax and cytochrome *c* translocations, cells were fractionated into cytosolic and membrane-bound organellar fractions using low concentrations of digitonin (42, 44, 68). Briefly, cells were incubated with 0.05% digitonin in an isotonic buffer for 2 minutes at room temperature. The digitonin soluble part was collected as the cytosolic fraction, and the insoluble part was further dissolved in 2% SDS to collect the membrane-bound organellar fraction. The collected subcellular fractions were subjected to electrophoresis and immunoblot analysis.

Transient transfection of RPTCs

Cells were plated at 0.5×10^6 cells per 35-mm dish to reach 50%–60% confluence after overnight growth. The cells were then transfected with 1 μg PKC plasmids (PKCδ-KD, PKCδ-CF, or PKCα-KD) using Lipofectamin 2000 (Invitrogen). To identify the transfected cells for analysis, 0.2 μg pEGFP-C3 was cotransfected. The cells were subjected to experimental treatment after 24 hours of transfection.

Renal function and histology

To monitor renal function, serum creatinine and BUN levels were determined using commercial kits as previously described (33–35). For histology, kidney tissues were fixed with 4% paraformaldehyde for paraffin embedding and H&E staining. Tissue damage was scored by the percentage of renal tubules with cell lysis, loss of brush border, and cast formation (0, no damage; 1, <25%; 2, 25%–50%; 3, 50%–75%; 4, >75%).

Measurement of cisplatin in tissues

Renal tissues were collected and homogenized for cisplatin measurement using flameless atomic absorption spectrometry as previously described (69).

Statistics

Qualitative data shown in this study, including immunoblots and cell and tissue images, are representative of at least 3 separate experiments. Quantitative data are expressed as mean ± SD. Student's *t* test was used to determine the statistical significance in the differences between 2 groups. One-way ANOVA followed by Tukey's post-hoc test was used to compare multiple treatment groups. Two-way ANOVA was used to assess the statistical significance of the differences between multiple treatment groups at different time points. Kaplan-Meier analysis (log-rank test) was used to record animal survival. Statistical analysis was performed using GraphPad Prism version software (GraphPad). $P < 0.05$ was considered to reflect significant differences.

Acknowledgments

We thank Thomas C. Hamilton, George Coukos, Bert Vogelstein, Jae-Won Soh, Fushin Yu, and Jian Yu for cancer cell lines, PKC plasmids, and anti-PUMA antibody. We thank Frank M. Balis and Robert F. Murphy (National Cancer Institute, Bethesda, Maryland, USA) for cisplatin measurement and Daria Mochly-Rosen (Stanford University School of Medicine, Stanford, California, USA) for information on δV1-1. We also thank Qingqing Wei, Patricia Scheonlein, and Vaishnavi Kundel at Georgia Health Sciences University for assistance in some experiments and Hongyan Xu for advice on statistics. The study was supported by grants from the NIH, Department of Veterans Affairs of USA, and the Cardiovascular Discovery Institute of Georgia Health Sciences University.

Received for publication October 28, 2010, and accepted in revised form April 6, 2011.

Address correspondence to: Zheng Dong, Department of Cellular Biology and Anatomy, Medical College of Georgia and Charlie Norwood VA Medical Center, 1459 Laney Walker Blvd., Augusta, Georgia 30912, USA. Phone: 706.721.2825; Fax: 706.721.6120; E-mail: zdong@mail.mcg.edu.

M. Vijay Kumar's present address is: VA Western New York Healthcare System, Buffalo, New York, USA.

1. Siddik ZH. Cisplatin: mode of cytotoxic action and molecular basis of resistance. *Oncogene*. 2003; 22(47):7265–7279.
2. Wang D, Lippard SJ. Cellular processing of platinum anticancer drugs. *Nat Rev Drug Discov*. 2005; 4(4):307–320.
3. Cepeda V, Fuertes MA, Castilla J, Alonso C, Quevedo C, Perez JM. Biochemical mechanisms of cisplatin cytotoxicity. *Anticancer Agents Med Chem*. 2007; 7(1):3–18.
4. Einhorn LH. Curing metastatic testicular cancer. *Proc Natl Acad Sci U S A*. 2002;99(7):4592–4595.
5. Launay-Vacher V, Rey JB, Isnard-Bagnis C, Deray G, Daouphars M. Prevention of cisplatin nephrotoxicity: state of the art and recommendations from the European Society of Clinical Pharmacy Special Interest Group on Cancer Care. *Cancer Chemother Pharmacol*. 2008;61(6):903–909.
6. Miller RP, Tadagavadi RK, Ramesh G, Reeves PG. Mechanisms of cisplatin nephrotoxicity. *Toxins*. 2010; 2(11):2490–2518.
7. Pabla N, Dong Z. Cisplatin nephrotoxicity: Mechanisms and renoprotective strategies. *Kidney Int*. 2008; 73(9):994–1007.
8. Price PM, Megyesi J, Safirstein RL. Cell cycle regulation: repair and regeneration in acute renal failure. *Semin Nephrol*. 2003;23(5):449–459.
9. Davis CA, Nick HS, Agarwal A. Manganese superoxide dismutase attenuates Cisplatin-induced renal injury: importance of superoxide. *J Am Soc Nephrol*. 2001;12(12):2683–2690.
10. Agarwal A, Balla J, Alam J, Croatt AJ, Nath KA. Induction of heme oxygenase in toxic renal injury: a protective role in cisplatin nephrotoxicity in the rat. *Kidney Int*. 1995;48(4):1298–1307.
11. Arany I, Megyesi JK, Kaneto H, Price PM, Safirstein RL. Cisplatin-induced cell death is EGFR/src/ERK signaling dependent in mouse proximal tubule cells. *Am J Physiol Renal Physiol*. 2004;287(3):F543–F549.
12. Baliga R, Zhang Z, Baliga M, Ueda N, Shah SV. In vitro and in vivo evidence suggesting a role for iron in cisplatin-induced nephrotoxicity. *Kidney Int*.

1998;53(2):394–401.
13. Kuwana H, et al. The phosphoinositide-3 kinase gamma-Akt pathway mediates renal tubular injury in cisplatin nephrotoxicity. *Kidney Int*. 2008; 73(4):430–445.
14. Liu H, Baliga R. Endoplasmic reticulum stress-associated caspase 12 mediates cisplatin-induced LLC-PK1 cell apoptosis. *J Am Soc Nephrol*. 2005; 16(7):1985–1992.
15. Megyesi J, Safirstein RL, Price PM. Induction of p21WAF1/CIP1/SDI1 in kidney tubule cells affects the course of cisplatin-induced acute renal failure. *J Clin Invest*. 1998;101(4):777–782.
16. Nowak G. Protein kinase C-alpha and ERK1/2 mediate mitochondrial dysfunction, decreases in active Na+ transport, and cisplatin-induced apoptosis in renal cells. *J Biol Chem*. 2002;277(45):43377–43388.
17. Park MS, De Leon M, Devarajan P. Cisplatin induces apoptosis in LLC-PK1 cells via activation of mitochondrial pathways. *J Am Soc Nephrol*. 2002;13(4):858–865.
18. Ramesh G, Reeves WB. TNF-alpha mediates chemokine and cytokine expression and renal injury in cisplatin nephrotoxicity. *J Clin Invest*. 2002; 110(6):835–842.
19. Ramesh G, Reeves WB. p38 MAP kinase inhibition ameliorates cisplatin nephrotoxicity in mice. *Am J Physiol Renal Physiol*. 2005;289(1):F166–F174.
20. Shiraishi F, et al. Heme oxygenase-1 gene ablation or expression modulates cisplatin-induced renal tubular apoptosis. *Am J Physiol Renal Physiol*. 2000;278(5):F726–F736.
21. Tsuruya K, et al. Direct involvement of the receptor-mediated apoptotic pathways in cisplatin-induced renal tubular cell death. *Kidney Int*. 2003;63(1):72–82.
22. Zhang B, Ramesh G, Uematsu S, Akira S, Reeves WB. TLR4 signaling mediates inflammation and tissue injury in nephrotoxicity. *J Am Soc Nephrol*. 2008; 19(5):923–932.
23. Yu F, Megyesi J, Safirstein RL, Price PM. Involvement of the CDK2-E2F1 pathway in cisplatin cytotoxicity in vitro and in vivo. *Am J Physiol Renal Physiol*. 2007;293(1):F52–F59.
24. Goligorsky MS. How to keep kidneys safe while shrinking tumors: the conundrum of cisplatin action. *Am J Physiol Renal Physiol*. 2007;293(1):F50–F51.
25. Gutcher I, Webb PR, Anderson NG. The isoform-specific regulation of apoptosis by protein kinase C. *Cell Mol Life Sci*. 2003;60(6):1061–1070.
26. Jackson DN, Foster DA. The enigmatic protein kinase Cdelta: complex roles in cell proliferation and survival. *FASEB J*. 2004;18(6):627–636.
27. Steinberg SF. Distinctive activation mechanisms and functions for protein kinase Cdelta. *Biochem J*. 2004;384(pt 3):449–459.
28. Steinberg SF. Structural basis of protein kinase C isoform function. *Physiol Rev*. 2008;88(4):1341–1378.
29. Basu A. Involvement of protein kinase C-delta in DNA damage-induced apoptosis. *J Cell Mol Med*. 2003; 7(4):341–350.
30. Brodie C, Blumberg PM. Regulation of cell apoptosis by protein kinase c delta. *Apoptosis*. 2003;8(1):19–27.
31. Reyland ME. Protein kinase Cdelta and apoptosis. *Biochem Soc Trans*. 2007;35(pt 5):1001–1004.
32. Faubel S, Ljubanovic D, Reznikov L, Somerset H, Dinarello CA, Edelstein CL. Caspase-1-deficient mice are protected against cisplatin-induced apoptosis and acute tubular necrosis. *Kidney Int*. 2004; 66(6):2202–2213.
33. Wei Q, Dong G, Franklin J, Dong Z. The pathological role of Bax in cisplatin nephrotoxicity. *Kidney Int*. 2007;72(1):53–62.
34. Wei Q, Dong G, Yang T, Megyesi J, Price PM, Dong Z. Activation and involvement of p53 in cisplatin-induced nephrotoxicity. *Am J Physiol Renal Physiol*. 2007;293(4):F1282–F1291.
35. Brooks C, Wei Q, Cho S, Dong Z. Regulation of mitochondrial dynamics in acute kidney injury in cell culture and rodent models. *J Clin Invest*. 2009; 119(5):1275–1285.
36. Ghayur T, et al. Proteolytic activation of protein kinase C delta by an ICE/CED 3-like protease induces characteristics of apoptosis. *J Exp Med*. 1996; 184(6):2399–2404.
37. DeVries-Seimon TA, Ohm AM, Humphries MJ, Reyland ME. Induction of apoptosis is driven by nuclear retention of protein kinase C delta. *J Biol Chem*. 2007;282(31):22307–22314.
38. Soltoff SP. Rottlerin: an inappropriate and ineffective inhibitor of PKCdelta. *Trends Pharmacol Sci*. 2007;28(9):453–458.
39. Chou WH, et al. Neutrophil protein kinase Cdelta as a mediator of stroke-reperfusion injury. *J Clin Invest*. 2004;114(1):49–56.
40. Cummings BS, Schnellmann RG. Cisplatin-induced renal cell apoptosis: caspase 3-dependent and -independent pathways. *J Pharmacol Exp Ther*. 2002; 302(1):8–17.
41. Jiang M, et al. Regulation of PUMA–alpha by p53 in cisplatin–induced renal cell apoptosis. *Oncogene*. 2006;25(29):4056–4066.
42. Jiang M, Yi X, Hsu S, Wang CY, Dong Z. Role of p53 in cisplatin-induced tubular cell apoptosis: dependence on p53 transcriptional activity. *Am J Physiol Renal Physiol*. 2004;287(6):F1140–F1147.
43. Seth R, Yang C, Kaushal V, Shah SV, Kaushal GP. p53-dependent caspase-2 activation in mitochondrial release of apoptosis-inducing factor and its role in renal tubular epithelial cell injury. *J Biol Chem*. 2005;280(35):31230–31239.
44. Pabla N, Huang S, Mi QS, Daniel R, Dong Z. ATR-Chk2 signaling in p53 activation and DNA damage response during cisplatin-induced apoptosis. *J Biol Chem*. 2008;283(10):6572–6583.
45. Jiang M, Dong Z. Regulation and pathological role of p53 in cisplatin nephrotoxicity. *J Pharmacol Exp Ther*. 2008;327(2):300–307.
46. Molitoris BA, et al. siRNA targeted to p53 attenuates ischemic and cisplatin-induced acute kidney injury. *J Am Soc Nephrol*. 2009;20(8):1754–1764.
47. Tsuruya K, et al. Involvement of p53-transactivated Puma in cisplatin-induced renal tubular cell death. *Life Sciences*. 2008;83(15–16):550–556.
48. Sheikh-Hamad D, et al. Cellular and molecular studies on cisplatin-induced apoptotic cell death in rat kidney. *Arch Toxicol*. 2004;78(3):147–155.
49. Jo SK, Cho WY, Sung SA, Kim HK, Won NH. MEK inhibitor, U0126, attenuates cisplatin-induced renal injury by decreasing inflammation and apoptosis. *Kidney Int*. 2005;67(2):458–466.
50. Liu M, et al. A pathophysiologic role for T lymphocytes in murine acute cisplatin nephrotoxicity. *J Am Soc Nephrol*. 2006;17(3):765–774.
51. Tadagavadi RK, Reeves WB. Renal dendritic cells ameliorate nephrotoxic acute kidney injury. *J Am Soc Nephrol*. 2010;21(1):53–63.
52. Zhang L, et al. Generation of a syngeneic mouse model to study the effects of vascular endothelial growth factor in ovarian carcinoma. *Am J Pathol*. 2002; 161(6):2295–2309.
53. Chen L, et al. Opposing cardioprotective actions and parallel hypertrophic effects of delta PKC and epsilon PKC. *Proc Natl Acad Sci U S A*. 2001; 98(20):11114–11119.
54. Qi X, Inagaki K, Sobel RA, Mochly-Rosen D. Sustained pharmacological inhibition of deltaPKC protects against hypertensive encephalopathy through prevention of blood-brain barrier breakdown in rats. *J Clin Invest*. 2008;118(1):173–182.
55. Bright R, et al. Protein kinase C delta mediates cerebral reperfusion injury in vivo. *J Neurosci*. 2004; 24(31):6880–6888.
56. Yoshida K, Liu H, Miki Y. Protein kinase C delta regulates Ser46 phosphorylation of p53 tumor suppressor in the apoptotic response to DNA damage. *J Biol Chem*. 2006;281(9):5734–5740.
57. Ryer EJ, et al. Protein kinase C delta induces apoptosis of vascular smooth muscle cells through induction of the tumor suppressor p53 by both p38-dependent and p38-independent mechanisms. *J Biol Chem*. 2005;280(42):35310–35317.
58. McCracken MA, Miraglia LJ, McKay RA, Strobl JS. Protein kinase C delta is a prosurvival factor in human breast tumor cell lines. *Mol Cancer Ther*. 2003; 2(3):273–281.
59. Wang Q, Wang X, Evers BM. Induction of cIAP-2 in human colon cancer cells through PKC delta/NF-kappa B. *J Biol Chem*. 2003;278(51):51091–51099.
60. Clark AS, West KA, Blumberg PM, Dennis PA. Altered protein kinase C (PKC) isoforms in non-small cell lung cancer cells: PKCdelta promotes cellular survival and chemotherapeutic resistance. *Cancer Res*. 2003;63(4):780–786.
61. Ringshausen I, Oelsner M, Weick K, Bogner C, Peschel C, Decker T. Mechanisms of apoptosis-induction by rottlerin: therapeutic implications for B-CLL. *Leukemia*. 2006;20(3):514–520.
62. Brenner W, et al. Migration of renal carcinoma cells is dependent on protein kinase Cdelta via beta1 integrin and focal adhesion kinase. *Int J Oncol*. 2008; 32(5):1125–1131.
63. De Servi B, Hermani A, Medunjanin S, Mayer D. Impact of PKCdelta on estrogen receptor localization and activity in breast cancer cells. *Oncogene*. 2005; 24(31):4946–4955.
64. Grossoni VC, Falbo KB, Kazanietz MG, de Kier Joffe ED, Urtreger AJ. Protein kinase C delta enhances proliferation and survival of murine mammary cells. *Mol Carcinog*. 2007;46(5):381–390.
65. Kiley SC, Clark KJ, Goodnough M, Welch DR, Jaken S. Protein kinase C delta involvement in mammary tumor cell metastasis. *Cancer Res*. 1999; 59(13):3230–3238.
66. Luo J, Solimini NL, Elledge SJ. Principles of cancer therapy: oncogene and non-oncogene addiction. *Cell*. 2009;136(5):823–837.
67. Yamamoto T, Matsuzaki H, Kamada S, Ono Y, Kikkawa U. Biochemical assays for multiple activation states of protein kinase C. *Nat Protoc*. 2006; 1(6):2791–2795.
68. Brooks C, et al. Bak regulates mitochondrial morphology and pathology during apoptosis by interacting with mitofusins. *Proc Natl Acad Sci U S A*. 2007; 104(28):11649–11654.
69. Pabla N, Murphy RF, Liu K, Dong Z. The copper transporter Ctr1 contributes to cisplatin uptake by renal tubular cells during cisplatin nephrotoxicity. *Am J Physiol Renal Physiol*. 2009;296(3):F505–F511.